

Studies of palladium electrodeposition from baths based on $\text{Pd}(\text{NH}_3)_2\text{X}_2$

Part II: $\text{X} = \text{Br}$ and $\text{X} = \text{NO}_2$

R. LE PENVEN, W. LEVASON, D. PLETCHER

Department of Chemistry, The University, Southampton SO9 5NH, UK

Received 20 June 1991; revised 20 August 1991

The chemistry and electrochemistry of electroplating baths based on $\text{Pd}(\text{NH}_3)_2\text{Br}_2$ and $\text{Pd}(\text{NH}_3)_2(\text{NO}_2)_2$ has been investigated and compared with that previously reported for $\text{Pd}(\text{NH}_3)_2\text{Cl}_2$. It is shown that electroactive species in all the baths is $\text{Pd}(\text{NH}_3)_4^{2+}$ and, hence, the mechanisms and current efficiencies for the cathodic deposition of palladium metal are similar in all three media. On the other hand, only in bromide electrolytes is the palladium found to dissolve anodically.

1. Introduction

Palladium is commonly electroplated from baths where one of the trans square planar palladium (II) complexes, $\text{Pd}(\text{NH}_3)_2\text{X}_2$ (X is Cl, Br or NO_2) is dissolved in an aqueous electrolyte containing ammonia and a buffer at a pH in the range 7–10 [1–6]. Fundamental studies of the chemistry and electrochemistry of these solutions are, however, very limited [7–9].

In the first paper of this series [10], we reported a study of a bath prepared from $\text{Pd}(\text{NH}_3)_2\text{Cl}_2$ and we now wish to report the extension of the investigation to the other complexes. The composition of the three solutions studied are shown in Table 1. They differ from typical commercial plating baths only in that the palladium concentration is low ($\approx 1.1 \text{ g dm}^{-3}$ compared to perhaps 5–20 g dm^{-3} in a commercial bath). It is also shown that the same solutions may be prepared directly from PdCl_2 and PdBr_2 .

2. Experimental details

The equipment and experimental procedures have been described previously [10]. All the palladium complexes and salts were supplied by Johnson Matthey.

3. Results

3.1. Spectroscopic studies

U.v.-visible spectra were recorded for each of the solutions in Table 1. All spectra, even when recorded immediately after preparation of the solutions, were similar; the major feature is an absorption peak, $\lambda_{\text{max}} = 293 \text{ nm}$ and extinction coefficient, $\epsilon \approx 190 \text{ cm}^{-1} \text{ dm}^3 \text{ mol}^{-1}$. There is also a weak shoulder at 353 nm. By comparison with solid state spectra and spectra reported in the literature [10–12], there can be no doubt that the palladium is present in solution as $\text{Pd}(\text{NH}_3)_4^{2+}$. It was also found that dissolution of

PdCl_2 or PdBr_2 in ammonia solutions in the pH range 8–11, led to the same spectrum. Therefore, it is concluded that the displacement of X by NH_3 in $\text{Pd}(\text{NH}_3)_2\text{X}_2$ is a rapid reaction and that a $\text{Pd}(\text{NH}_3)_4^{2+}$ solution may be prepared by dissolving one of many palladium compounds in an ammonia based buffer. In the case of $\text{Pd}(\text{NH}_3)_2(\text{NO}_2)_2$, the substitution will be further enhanced by the reaction of free nitrite with the excess ammonia to give nitrogen in the bath.

3.2. Electrochemical studies

Figure 1a and b show slow sweep cyclic voltammograms recorded at a vitreous carbon RDE, $\omega = 400 \text{ r.p.m.}$, for solutions B and C deoxygenated with a fast stream of nitrogen. Also shown are the $I-E$ curves for the aqueous buffers without palladium (II) at a palladium plated vitreous carbon RDE (the palladium layer was deposited by applying -800 mV/SCE while a charge of 0.1 C cm^{-2} was passed in the solution under study).

With the bromide solution, the forward scan shows only a very low current positive to -850 mV . Thereafter, the current increases and reaches a shoulder around -1100 mV before hydrogen evolution commences. A better formed reduction wave is seen on the reverse scan, $E_{1/2} = -780 \text{ mV}$. Also, as expected for an electrode reaction involving the deposition of a metal onto a carbon substrate, there is a potential range where the cathodic current is much higher on the reverse sweep than on the forward one. The reverse scan also shows an anodic current positive to -500 mV and a large symmetrical peak centred around $+300 \text{ mV}$. The response for solution C is very similar to that reported for the chloride medium, solution A [10]. They differ markedly from the response in the bromide medium only in one respect; the large anodic peak at $+300 \text{ mV}$ is absent. In all solutions, a broad anodic peak is observed just positive to -500 mV and this is associated with hydrogen

Table 1. Palladium electroplating solutions discussed in this paper.

Bath	X	[Pd(II)]/mmol dm ⁻³	Electrolytes	pH
A	Cl	10	1 mol dm ⁻³ NH ₄ Cl	8.9
B	Br	10	1 mol dm ⁻³ NH ₄ Br	8.5
C	NO ₂	14	1 mol dm ⁻³ (NH ₄) ₂ HPO ₄ + 1 mol dm ⁻³ NH ₃	10.2

desorption from the palladium lattice [10]. On the other hand, only in the bromide medium is the total anodic charge of the same magnitude as the total cathodic charge. This suggests that the palladium metal redissolves anodically in the bromide solution. Indeed, in contrast to the other solutions, no palladium can be seen on the carbon surface at the end of the voltammogram and, thereafter, the electrode has the properties of vitreous carbon not palladium.

The cathodic currents negative to -800 mV are strongly dependent on the rotation rate of the disc and when the steady state currents at -1000 mV are plotted as a function of the square root of rotation rate, straight lines passing through the origin are obtained, confirming that the electrode is largely mass transport

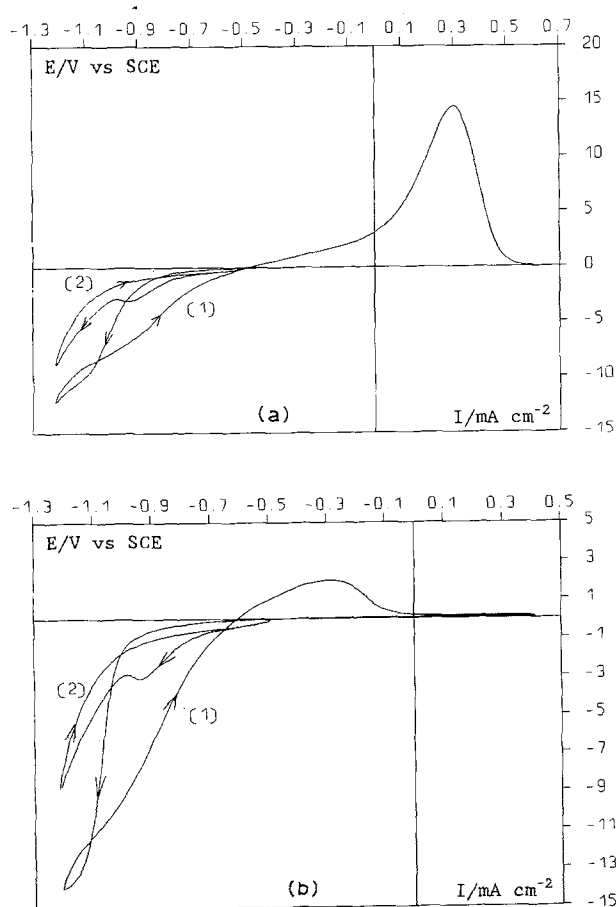
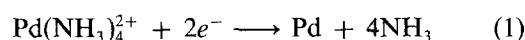
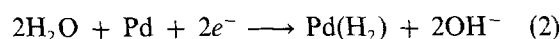


Fig. 1. I - E curves recorded at a disc electrode rotating at 400 r.p.m. and using a potential scan rate of 20 mV s^{-1} . (a) curve 1: vitreous carbon electrode in bath B. curve 2: palladium plated vitreous carbon in the electrolyte of bath B but without Pd(II). (b) curve 1: vitreous carbon electrode in bath C. curve 2: palladium plated vitreous carbon in the electrolyte of bath C but without Pd(II).

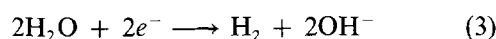
controlled. When it is assumed that the only electrode reaction is



the values for the diffusion coefficient found for Pd(II) in baths A, B and C are 10.2×10^{-6} , 11.4×10^{-6} and $11.8 \times 10^{-6} \text{ cm}^2 \text{ s}^{-1}$, respectively. These values are somewhat higher than expected ($5-7 \times 10^{-6} \text{ cm}^2 \text{ s}^{-1}$) and the cyclic voltammograms in the absence of palladium (II), see Fig. 1a and b, clearly show that competing electrode reactions are occurring at this potential. These include

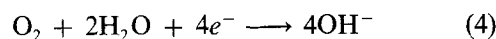


and



Reaction 2 is clearly seen as a peak around -900 mV on the responses for the palladium electrode in the buffers (*i.e.* curves 2 in Fig. 1a and b); the reverse, desorption reaction leads to the anodic peaks at ≈ -300 mV. Reaction 3 is seen as a steep rise in current beyond -1100 mV.

A series of experiments were then carried out with solutions B and C to determine the relative importance of Reactions 1-3 and also oxygen reduction



as a function of potential in the plating baths in equilibrium with air (as used in commercial practice). The following experiments were carried out at a stationary electrode in unstirred solution:

(i) slow potential sweep experiments at a palladium plated disc electrode for the air equilibrated solutions show two reduction waves, $E_{1/2} \approx -100$ and -400 mV for the stepwise reduction of oxygen. The potential of this electrode was stepped from 0 to -550 mV and the steady state current was estimated after 100 s. Since this potential is within the mass transport limited plateau, it was assumed that this current, I_4 , would be observed at all potentials more negative than -500 mV.

(ii) The potential of a polished vitreous carbon disc electrode in the plating solutions was stepped from -500 mV to a value, E_D , in the range -740 to -900 mV. The current, after the passage of 0.1 C cm^{-2} , has reached a steady state value and results from the electrode reactions, Equations 1-4, (*i.e.* $I = I_1 + I_2 + I_3 + I_4$). Typically the length of this pulse is 100-200 s.

(iii) At the end of this pulse, the potential was stepped back to -500 mV and the anodic charge at this potential results only from the desorption of hydrogen from the palladium lattice. The average current for Reaction 2, I_2 , during the metal deposition step may be estimated by dividing this anodic charge by the length of the pulse at E_D .

(iv) The palladium plated carbon disc was then washed well and transferred to deoxygenated buffer

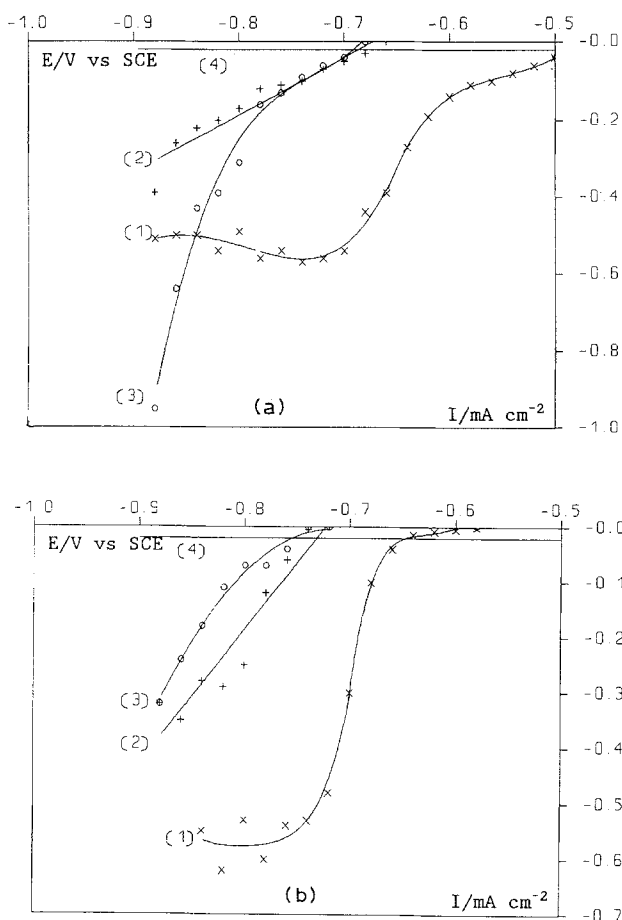


Fig. 2. Partial current densities as a function of potential for (1) palladium deposition (2) hydrogen absorption (3) hydrogen evolution and (4) oxygen reduction in an unstirred, air equilibrated plating bath. (a) bath B, (b) bath C.

solution without Pd(II). The potential sequence $-500 \text{ mV} \rightarrow E_D \rightarrow -500 \text{ mV}$ was repeated using the same pulse time at E_0 as in (ii) above. The current at the end of the pulse at E_0 is $I_3 + I_4$. The anodic charge during the pulse at -500 mV provides a check as to the extent of hydrogen absorption into the palladium lattice.

This data allows the values of I_1 , I_2 , I_3 and I_4 each to be computed. The range of E_D which can be investigated was extended as follows: (i) between -640 mV and -740 mV , a short prepulse at -900 mV was used to ensure nucleation of the palladium lattice prior to the application of E_D (ii) for even less negative potentials, the palladium layer was grown at -650 mV until 0.1 C cm^{-2} had passed and the potential was then taken to the value of interest (note that before -650 mV , Reactions 2 and 3 do not occur significantly). Figure 2a and b report the partial currents for Reactions 1–4 over a range of potentials for solutions B and C. The corresponding plot for bath A is Fig. 8 in [10]. It can be seen that for all three baths, it is possible to find a range of potentials where oxygen reduction is the only competing reaction to palladium deposition. There appears to be a small difference in

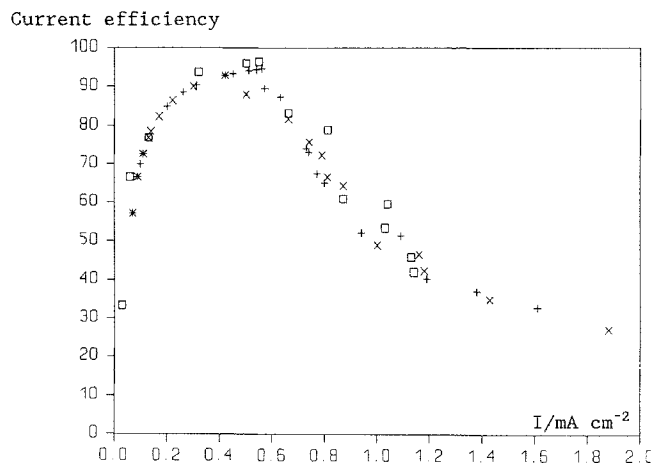


Fig. 3. Current efficiency versus current density for unstirred electroplating baths. (+) bath A, (x) bath B, (□) bath C.

the potentials for the deposition on palladium; the 'half wave potentials' taken from Fig. 2 and Fig. 8 in [10] are -570 , -640 and -700 mV for solutions A, B and C, respectively.

4. Discussion

The deposition of palladium from these plating baths seems to be a very straightforward process. The only detectable palladium species in the three solutions A, B and C is the same, $\text{Pd}(\text{NH}_3)_2^{2+}$, and, hence, substitution of X by NH_3 in the trans complexes, $\text{Pd}(\text{NH}_3)_2\text{X}_2$, appears to take place rapidly. Moreover, $\text{Pd}(\text{NH}_3)_4^{2+}$ seems to be reduced directly to the metal in the Reaction 1. At sufficiently negative potentials, Reaction 1 becomes mass transport controlled. Only small differences between the rates of the metal deposition reaction as a function of potential in the three solutions are observed, see for example Fig. 2a and b, and these should be attributed to differences between the electrolyte properties and not a change in the electroactive species. The electrolyte pH is not identical in the three baths and there could also be weak interactions between the palladium cation and the different anions of the electrolyte.

Figure 3 shows the data of Fig. 2 (and Fig. 8 in [10]) replotted to show current efficiency as a function of current density. It can again be seen that the three baths give very similar data. Commercial operation should always use a current density below the drop-off in current efficiency since the first competing reaction (excluding oxygen reduction, which always occurs) will be hydrogen absorption into the palladium lattice and this may well lead to stress and other unwanted characteristics. At and below the maximum, however, this unwanted reaction does not contribute to the current.

The similarity in the rates of deposition and the current efficiency does not necessarily imply that deposit properties will be identical from the three baths; ions such as nitrite could act as additives and modify the characteristics of the palladium layer. On the other hand, since the palladium species in the bath

does not depend on the source of palladium, clearly the cheapest should be used. If desirable, the bath may be modified by other additions (eg. nitrite could be added as sodium nitrite).

It should be emphasised that Fig. 3 is drawn for a palladium concentration (10 mmol dm^{-3} or 1.1 g dm^{-3}) low compared with commercial plating baths. With increasing palladium (II) concentration, there will be a slight increase in current efficiency (both oxygen reduction and hydrogen evolution will become less important) but the general shape of the curve will be retained. Moreover, the current density for maximum current efficiency will be almost proportional to Pd(II) concentration. It is also clear that a large increase in deposition rate could be achieved, without loss in current efficiency, by introducing convection into the bath. Figure 3 is drawn for an unstirred electrolyte and, in a bath with efficient stirring or flowing electrolyte, the current density could be increased by more than an order of magnitude while only the electrode Reactions 1 and 4 would take place.

The palladium stripping peak in the bromide medium introduces another possibility into the technology of palladium plating. A bromide bath could be operated with a dissolving anode (this is also possible in more acidic baths). A bromide electrolyte may also be suitable for (a) the electrostripping and recovery of metal from redundant palladium plated components and (b) the coulometric determination of the thickness

of palladium plates.

Acknowledgement

The authors would like to thank Johnson Matthey Materials Technology Division, Royston, Hertfordshire, for financial support of this work. They are also most grateful to Mr Peter Skinner for his advice and encouragement throughout the programme.

References

- [1] R. F. Vines, R. H. Atkinson and F. H. Reid, in 'Modern Electroplating', (edited by F. A. Lowenheim), Wiley, New York (1974).
- [2] H. D. Hedrich and Ch. J. Raub, *Metaloberfläche* **31** (1977) 512.
- [3] Ch. J. Raub, *Platinum Metals Rev.* **26** (1982) 158.
- [4] R. J. Morrissey, *ibid.* **27** (1983) 10.
- [5] Y. Fukumoto, Y. Kawashima, K. Handa and Y. Hayashi, *Met. Finish.* **84** (1984) 77.
- [6] S. Jayakrishnan and S. R. Natarajan, *Met. Finish.* **88** (1988) 81.
- [7] H. D. Hedrich and Ch. J. Raub, *Surf. Technol.* **8** (1979) 347.
- [8] M. F. Bell and J. A. Harrison, *J. Electroanal. Chem.* **41** (1973) 15.
- [9] J. N. Crosby, J. A. Harrison and T. A. Whitfield, *Electrochim. Acta* **27** (1982) 897.
- [10] R. Le Penven, W. Levason and D. Pletcher, *J. Appl. Electrochem.* **20** (1990) 399.
- [11] A. J. Poe and D. H. Vaughan, *Inorg. Chem. Acta* **1** (1967) 255.
- [12] L. Rasmussen and C. K. Jorgensen, *Acta Chem. Scand.* **22** (1968) 2313.